# Measurement of electron-hole friction in an n-doped GaAs/AlGaAs quantum well using optical transient-grating spectroscopy

Luyi Yang,[1,2] J. D. Koralek,[1,2] J. Orenstein*,[1,2] D. R. Tibbetts,[3] J. L. Reno,[3] and M. P. Lilly[3]

[1]*Department of Physics, University of California, Berkeley, California 94720, USA.*
[2]*Materials Science Division, Lawrence Berkeley National Laboratory, Berkeley, California 94720, USA.*
[3]*Sandia National Laboratories, Albuquerque, New Mexico 87123, USA.*

(Dated: April 27, 2011)

We use phase-resolved transient grating spectroscopy to measure the drift and diffusion of electron-hole density waves in a semiconductor quantum well. The unique aspects of this optical probe allow us to determine the frictional force between a two-dimensional Fermi liquid of electrons and a dilute gas of holes. Knowledge of electron-hole friction enables prediction of ambipolar dynamics in high-mobility electron systems.

PACS numbers: 78.47.jj, 73.63.Hs

The motion of electrons and holes is crucial to the operation of virtually all semiconductor devices and is a central topic of the classic semiconductor texts [1, 2]. In particular the coupled motion of electron-hole ($e$-$h$) packets in applied electric fields, known as ambipolar transport, is discussed in depth. However, it has been known for some time, although not perhaps widely appreciated, that the motion of $e$-$h$ packets in the high-mobility electron gases found in semiconductor quantum wells and heterojunctions violates the predictions of the standard theory. Insufficient understanding of ambipolar dynamics poses a problem for the development of a spin-based electronics, as many prospective devices are based on spin currents carried by spin polarized $e$-$h$ packets subjected to electric fields [3–5].

In the standard textbook description of ambipolar transport in a doped semiconductor, electrons and holes interact only through the long-range Coulomb interaction. Momentum relaxation occurs by scattering on impurities and phonons and there is no exchange of momentum between electrons and holes. On the basis of these assumptions it is predicted that in an n-type semiconductor, for example, an $e$-$h$ packet drifts in direction of the force on the holes, opposite to the motion of the Fermi sea of electrons. However, by photoluminescence imaging, Höpfel *et al.* discovered that in GaAs quantum wells a drifting $e$-$h$ packet moves in the direction of the majority, rather than minority carrier, an effect they termed "negative ambipolar mobility" [6]. They recognized that this effect originates from the scattering between electrons and holes, neglected in the standard versions of ambipolar transport.

The scattering that dominates ambipolar transport in a single quantum well is precisely analogous to the Coulomb drag effect that has been studied intensively in systems in which layers of electron gases are in close proximity [7–9]. In such systems, the strength of the Coulomb interaction between layers can be determined with precision via the transresistance, which is the ratio of the voltage induced in one layer to a current in the other . The transresistance is a direct measure of the rate of momentum exchange (or frictional force) between the two coupled electronic systems. Unfortunately, this technique cannot be used to probe the much stronger frictional force between electrons and holes in the same layer, which plays a crucial role in ambipolar dynamics.

In the experiments reported here we perform the first complete characterization of coupled $e$-$h$ transport in a two-dimensional electron gas (2DEG) by measuring simultaneously the ambipolar diffusion coefficient, $D_a$ and the ambipolar mobility, $\mu_a$. From these measured coefficients, and a simple model of momentum exchange between the Fermi sea and the packet, we obtain the effective drag resistance $\rho_{eh}$ between electrons and holes in a single quantum well. We show that the value of $\rho_{eh}$ for a single layer, although orders of magnitude larger the transresistance of bilayers, can be quantitatively understood using the same random-phase approximation (RPA) model that describes coupled quantum wells. Based on these findings, it becomes possible to predict the ambipolar transport coefficients for high-mobility semiconductors as a function of carrier density and temperature.

Our measurements of $e$-$h$ transport are performed using transient grating spectroscopy (TGS) [10], which is a contact-free technique based on time-resolved optics. In TGS standing waves of either $e$-$h$

*To whom all correspondence should be addressed. Email: jworenstein@lbl.gov

or spin density [11] are created in a 2DEG by photoexcitation with two non-collinear beams of light from a pulsed (100 femtosecond) laser. When the pulses are polarized in the same direction, interference generates a standing wave of laser intensity, creating a sinusoidal pattern of *e-h* density whose spatial period depends on the angle between the interfering beams. The *e-h* density wave imprinted in the 2DEG induces local variation in the index of refraction, and therefore acts as an optical diffraction grating. The time evolution of the density waves after pulsed photogeneration can be monitored via the diffraction of a time-delayed probe pulse.

The ambipolar diffusion coefficient can be readily determined by measuring the rate at which the grating amplitude decays as a function of its wavelength. However, as we discuss below, characterization of $\rho_{eh}$ requires that $\mu_a$ must also be measured under the same experimental conditions. The latter is the coefficient that relates the drift velocity of the *e-h* density wave to the magnitude of an electric field, $E$, applied in the plane of the 2DEG. Measurement of $\mu_a$ clearly requires sensitivity to the position of the *e-h* density wave - information that is contained in the *phase shift* of the diffracted light. On the other hand, conventional scattering experiments measure light intensity, and thus phase information is lost. In the experiments reported here, we demonstrate that time-resolved detection of both *amplitude and phase* of light diffracted from a drifting *e-h* density wave allows simultaneous determination $\mu_a$ and $D_a$, which together yield the transresistance of the coupled *e-h* system.

The measurements were performed on a 9 nm wide n-doped GaAs/AlGaAs quantum well (QW), grown by molecular beam epitaxy on a semi-insulating GaAs (001) substrate (VB0355). The carrier density and mobility of the 2DEG are $1.9 \times 10^{11}/\text{cm}^2$ and $5.5 \times 10^5 \text{cm}^2/\text{V-s}$ at 5 K, respectively. The silicon donors were symmetrically doped in the center of each barrier. The 2DEG channel was defined by a mesa etching, and ohmic contact was made by annealing NiGeAu to the sample. After patterning the GaAs substrate was mechanically lapped and chemically etched to allow for optical measurement in transmission geometry. Several samples were prepared with semi-transparent front and back gate electrodes to allow for continuous variation of the equilibrium electron density.

The electron-hole density grating was generated by focusing the two pump beams onto a 150 micron diameter spot between the two ohmic contacts, which are separated by 200 microns. Phase-sensitive detection of the light diffracted from the grating was

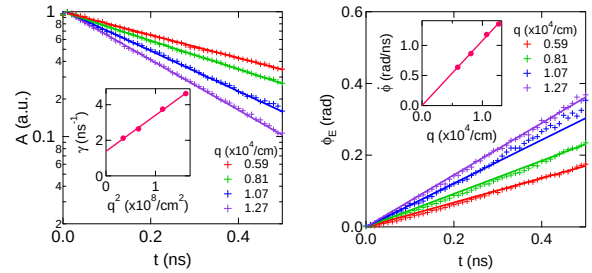


(a) (b)

FIG. 1: (Color online) (a) Relative amplitude of *e-h* density wave as function of time for several values of the wavevector, $q$, measured at 50 K. Inset: the decay rate, $\gamma$, of the amplitude, plotted as a function of $q^2$; the slope of the solid line through the data points is the ambipolar diffusion coefficient $D_a$ and the intercept is the inverse of the *e-h* recombination time $\tau_{rec}$. (b) Linear advance of the phase of the *e-h* density wave with time for several values of $q$, at 50 K. The applied electric field is $E \approx 2$V/cm. Inset: the rate of phase change $\dot{\phi}$ as a function of $q$.

performed using a heterodyne technique [12–17], in which scattered pulses are mixed in a Si photodiode with a beam of transmitted pulses acting as a local oscillator (LO). The output voltage of the Si detector contains a phase-sensitive term, proportional to $A(q,t)\exp[i(\phi_{pld} + \phi_E)]$, where $A(q,t)$ is the amplitude of the density wave, $\phi_{pld} = kd$ reflects the path length difference, $d$, between the LO and diffracted beams ($k$ is the wavevector of the light), and $\phi_E = \boldsymbol{q}\cdot\delta\boldsymbol{r}$, where $\boldsymbol{q}$ and $\delta\boldsymbol{r}$ are the grating wavevector and position, respectively. For uniform motion with velocity $\boldsymbol{v}$ parallel to $\boldsymbol{q}$, $\phi_E = qvt$. The linear advance of phase with time is equivalent to a Doppler shift of frequency, $\Delta\omega = qv$. The phase noise level of 0.01 radian in our detection system corresponds to an uncertainty in velocity of $\sim 10$ m/s, which is approximately four orders of magnitude smaller than the Fermi velocity $v_F$.

To measure $A(q,t)$ and $\phi_E(q,t)$ separately, we combine heterodyne detection with two phase-modulation schemes. To obtain $A(q,t)$ we modulate $\phi_{pld}$ by oscillating the angle of a coverslip placed in the LO beam path. For weak phase modulation the synchronously detected heterodyne signal is proportional to $A(q,t)\Delta\phi_{pld}$. To obtain $\phi_E(q,t)$ we oscillate the in-plane $E$-field (applied parallel to $\boldsymbol{q}$) that induces drift and measure the synchronous signal $A(q,t)v(E)qt$. From these two measurements we extract $A(q,t)$ and $qv(E)t$ independently.

In Fig. 1(a) we show the grating amplitude at a representative temperature of 50 K as a function of time after photogeneration, plotted on semi-log axes,

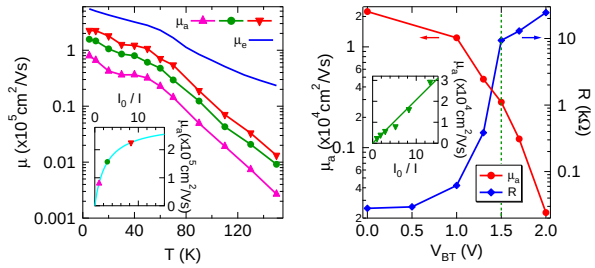


(a) (b)

FIG. 2: (Color online) (a) Ambipolar mobility $\mu_a$ at three different pump intensities compared with electron mobility $\mu_e$, as a function of $T$. Inset: $\mu_a$ as a function of laser intensity at 5 K, the solid line is a fit (see text). (b) Ambipolar mobility $\mu_a$ and sample resistance $R$ as a function of gate voltage $V_{BT}$ at 50 K. Inset: $\mu_a$ as a function of laser intensity at fixed gate bias $V_{BT}$=1.5V at 50 K; solid line is a linear fit showing that $\mu_a \propto 1/I$.

for several values of the grating wavevector. The decay of $A(q,t)$ is a single exponential with a rate constant, $\gamma$, that increases with increasing wavevector. As shown in the inset, $\gamma$ varies with $q$ as expected for the combined effects of diffusion and electron-hole recombination, $\gamma(q) = 1/\tau_{rec} + D_a q^2$, where $\tau_{rec}$ is the electron-hole recombination time.

In Fig. 1(b) we plot the phase of the $e$-$h$ density wave, $\phi_E(q,t)$ vs. $t$ for different values of $q$ at 50 K at full laser intensity $I_0 \simeq 0.25\mu$J-cm$^{-2}$ per pulse. The linear dependence of $\phi_E(q,t)$ on both $t$ and $q$ (see inset) is consistent with the Doppler shift $\phi_E(q,t) = v(E)qt$. The sign of the phase shift gives the direction of motion under the influence of the electric field, which we determine to be the same as that of the electron Fermi sea. From $\partial\phi_E(q,t)/\partial q$ at fixed time delay we obtain the drift velocity of the $e$-$h$ density wave. Normalizing by the applied electric field yields the ambipolar mobility, $\mu_a$.

In the course of the measurements we discovered that $\mu_a$ depends strongly on $I$, in addition to the expected dependence on temperature, $T$. Figure 2(a) shows $\mu_a$ determined using the analysis outlined above as a function of $T$, for three different values $I$. For comparison, we also plot the electron mobility, $\mu_e$, as determined from standard four-contact dc transport measurement. As is clear from Fig. 2(a), $\mu_a$ decreases when either $T$ or $I$ increase. When non-equilibrium laser experiments show such dependencies, there can be ambiguity as to whether the dependence on $I$ reflects an intrinsic dependence on the photogenerated carrier density, $\Delta n$, or the effect of transient local heating of the electron gas. To determine whether the $I$ dependence is intrinsic, we performed TGS measurements on a device with semi-transparent gate electrodes, which allowed us to vary the equilibrium electron density, $n_0$, at fixed $\Delta n$.

In Figure 2(b) we plot $\mu_a$ and the 2DEG resistance, $R$, at 50 K, as a function of the voltage between the two gates, $V_{BT}$. Clearly $\mu_a$ decreases rapidly as $n_0$ is driven to zero (and $R \to \infty$) by increasingly positive $V_{BT}$. As these measurements are performed at constant $I$, it is evident that the intensity dependence shown in Fig. 2(a) reflects an intrinsic dependence of $\mu_a$ on the ratio $\Delta n/n_0$, rather than laser-induced heating. The inset to Fig. 2(b) illustrates that $\mu_a$ scales as $1/I$ (equivalent to $1/\Delta n$) in regime where $n_0$ is small, while the Fig. 2(a) inset shows that $\mu_a$ approaches an asymptotic value $\mu_{a0}$ in the limit that $I$ (and $\Delta n$) $\to 0$. The overall dependence of variation of $\mu_a$ can be summarized by the simple formula,

$$\mu_a(I) = \frac{\mu_{a0}}{1 + \alpha(\Delta n/n_0)}, \tag{1}$$

where $\alpha$ is $T$ dependent parameter.

At this point, we can summarize our experimental findings as follows: (1) the photogenerated $e$-$h$ packet drifts under the influence of an $E$ field in the same direction as the Fermi sea of electrons, (2) the velocity of the packet goes to zero as $\Delta n/n_0 \to \infty$ and approaches a constant in the limit that $\Delta n/n_0 \to 0$, (3) the asymptotic value, $\mu_{a0}(T)$ [Fig. 3(a)] is proportional to, but slightly smaller than the electron mobility for $T < 80$ K, but becomes much smaller than $\mu_e$ for $T > 80$ K. Below we show below that each of these observations can be understood with a relatively simple model that treats the $e$-$h$ packet as a neutral gas of particles that can exchange momentum with the Fermi sea.

The stationary transport equations for free electrons and the packet can be written:

$$\frac{n_0 m_e v_e}{\tau_e} + n_0 \Delta n \gamma (v_e - v_p) = -n_0 e E,$$
$$\frac{\Delta n m_p v_p}{\tau_p} + n_0 \Delta n \gamma (v_p - v_e) + k_B T \nabla(\Delta n) = 0,$$

where $1/\tau_{e(p)}$ is the rate at which electrons(packet) lose momentum to the lattice, $m_e$ and $m_p$ are respective masses, and $\gamma$ is a parameter describing the rate of momentum exchange. By solving these equations we obtain precisely the form of Eq. 1, where,

$$\mu_{a0} = -\frac{\mu_e}{1 + \frac{\mu_e}{\mu_p}\frac{\rho_e}{\rho_{eh}}}, \tag{2}$$

and $\alpha = \mu_{a0}/\mu_p$. In Eq. 2 we have made use of the definitions, $\mu_p \equiv e\tau_p/m_p$, $\rho_e \equiv (n_0 e \mu_e)^{-1}$, and

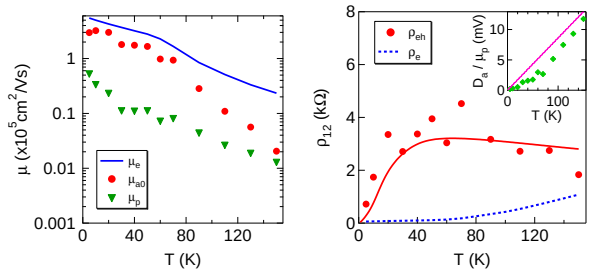


(a) (b)

FIG. 3: (Color online) (a) Comparison of electron mobility $\mu_e$; ambipolar mobility $\mu_{a0}$, and packet mobility $\mu_p$, as a function of $T$. (b) The $e$-$h$ drag transresistivity, $\rho_{eh}$, as a function of $T$; solid line is a theoretical prediction of $\rho_{eh}$ based on the RPA. Inset: $D_a/\mu_p$ compared with the Einstein relation prediction in the non-degenerate regime $k_BT/e$.

$\gamma \equiv e^2\rho_{eh}$. The negative sign of $\mu_a$ corresponds to the $e$-$h$ packet drifting in the same direction as the Fermi sea of electrons. In addition, we find that solving for the ambipolar diffusion coefficient yields,

$$D_a = \frac{k_BT\mu_{a0}}{e}\frac{\rho_e}{\rho_{eh}}. \tag{3}$$

From Eq. 3 we see that independent measurement of $\mu_{a0}$, $D_a$, and $\rho_e$ directly yields the electron-hole transresistance, $\rho_{eh}$. The values of $\rho_{eh}$ thus determined are plotted vs. $T$ in the Fig. 3(b), together with $\rho_e$ for comparison. We see that in the low $T$ regime, $\rho_e \ll \rho_{eh}$, which translates to an ambipolar mobility that is not too different from the electron mobility. As $T$ increases and $\rho_e$ approaches $\rho_{eh}$, $\mu_{a0}$ tends towards the much smaller $\mu_p$. While the values of ambipolar mobility are controlled by $\rho_e/\rho_{eh}$, $D_a$ itself is fairly insensitive to Coulomb drag because diffusive spreading of the packet takes place with parallel transport of electrons and holes. This effect is illustrated in the Fig. 3(b) inset, which compares the ratio $D_a/\mu_p$ to $k_BT/e$. The near agreement with the Einstein relation shows that $D_a$ is essentially determined by the non-degenerate gas of holes because the electrons in the packet are tethered to them through the long-range Coulomb interaction.

The values of $\rho_{eh}(T)$ that we obtain several orders of magnitude larger than those obtained in Coulomb drag experiments on coupled quantum wells [18, 19]. However, in the experiments reported here ($i$) electrons and holes are confined to the same quantum well and ($ii$) one of the Fermi gases (the holes) are non-degenerate throughout the $T$-range of the experiment. To test whether the values of $\rho_{eh}(T)$ shown in Fig. 3(b) are reasonable, we apply the standard RPA model for Coulomb drag to the single layer case. The RPA expression for $\rho_{eh}(T)$ is the phase space integral of the product of the interaction, $V_{\rm RPA}(q)$, and $\Im\{\chi_{1,2}\}$, the imaginary part of the susceptibility of fermion species 1 and 2, respectively [20–22]. To apply this theory to our experiment, we substitute the non-degenerate Lindhard response for the hole susceptibility [23]. Numerical evaluation of the phase space integral, plotted as solid line in Fig. 3(b), shows that the RPA interaction describes the experimental data quite well without any free parameters.

In conclusion, we have used phase-resolved TGS to simultaneously measure the ambipolar drift and diffusion of photoinjected electrons and holes. From these measurements we determine for the first time the frictional force between a degenerate Fermi liquid of electrons and a dilute gas of holes in the same two dimensional system. The measured values of $\rho_{eh}$ data are accurately described by the static limit of RPA-based theory with no free parameters. By combining $\rho_{eh}$ with a simple model based on conservation of momentum, the ambipolar dynamics of high-mobility electron gases can be predicted, enabling more powerful modeling of devices, for example those based on spin current of drifting polarized carriers.

This work was supported by the Director, Office of Science, Office of Basic Energy Sciences, Materials Sciences and Engineering Division, of the U.S. Department of Energy under Contract No. DE-AC02-05CH11231. Sample perparation was performed at the Center for Integrated Nanotechnologies, a U.S. Department of Energy, Office of Basic Energy Sciences user facility at Sandia National Laboratories (Contract DE-AC04-94AL85000).

**DISCLAIMER**

This document was prepared as an account of work sponsored by the United States Government. While this document is believed to contain correct information, neither the United States Government nor any agency thereof, nor the Regents of the University of California, nor any of their employees, makes any warranty, express or implied, or assumes any legal responsibility for the accuracy, completeness, or usefulness of any information, apparatus, product, or process disclosed, or represents that its use would not infringe privately owned rights. Reference herein to any specific commercial product, process, or service by its trade name, trademark, manufacturer, or otherwise, does not necessarily constitute or imply its endorsement, recommendation, or favoring by the United States Government or any agency thereof, or the Regents of the University of California. The views and opin-

ions of authors expressed herein do not necessarily state or reflect those of the United States Government or any agency thereof or the Regents of the University of California.

[1] S.M. Sze and K.K. Ng, *The Physics of Semiconductor Devices*, (John Wiley and Sons, New York, 2003).
[2] D.A. Neamen, *Semiconductor Physics and Devices: basic principles* 3rd ed. Ch. 6 (McGraw-Hill Higher Education, Boston, 2003).
[3] I. Zutic, J. Fabian, and S. Das Sarma, Rev. Mod. Phys. **76**, 323 (2004).
[4] J. Fabian, A. Matos-Abiague, C. Ertler, P. Stano, and I. Žutić, Acta Phys. Slov. **57**, 565 (2007).
[5] D.D. Awschalom and M.E. Flatté, Nature Phys. **3**, 153 (2007).
[6] R.A. Höpfel, J. Shah, P.A. Wolff, and A.C. Gossard, Phys. Rev. Lett. **56**, 2736 (1986).
[7] P.J. Price, Physica B & C **117**, 750 (1983).
[8] T.J. Gramila, J.P. Eisenstein, A.H. MacDonald, L.N. Pfeiffer, and K.W. West, Phys. Rev. Lett. **66**, 1216 (1991).
[9] U. Sivan, P.M. Solomon, and H. Shtrikman, Phys. Rev. Lett. **68**, 1196 (1992).
[10] H.J. Eichler, P. Gunter, and D.W. Pohl, *Laser-Induced Dynamic Gratings* (Springer-Verlag, Berlin, 1986).
[11] A.R. Cameron, P. Riblet, and A. Miller, Phys. Rev. Lett. **76**, 4793 (1996).
[12] P. Vohringer and N.F. Scherer, J. Phys. Chem. **99**, 2684 (1995).
[13] Y.J. Chang, P. Cong, and J.D. Simon, J. Phys. Chem. **99**, 7857 (1995).
[14] G.D. Goodno, G. Dadusc, and R.J.D. Miller, J. Opt. Soc. Am. B **15**, 1791 (1998).
[15] A.A. Maznev, K.A. Nelson, and J.A. Rogers, Opt. Lett. **23**, 1319 (1998).
[16] N. Gedik and J. Orenstein, Opt. Lett. **29**, 2109 (2004).
[17] N. Gedik, J. Orenstein, R. Liang, D.A. Bonn, and W.N. Hardy, Science **300**, 1410 (2003).
[18] A.F. Croxall *et al.*, Phys. Rev. Lett. **101**, 246801 (2008).
[19] J.A. Seamons, C.P. Morath, J.L. Reno, and M.P. Lilly, Phys. Rev. Lett. **102**, 026804 (2009).
[20] L. Zheng and A.H. MacDonald, Phys. Rev. B **48**, 8203 (1993).
[21] K. Flensberg and B.Y.-K. Hu, Phys. Rev. B **52**, 14796 (1995).
[22] G. Vignale and A.H MacDonald, Phys. Rev. Lett. **76**, 2786 (1996).
[23] G.F. Giuliani and G. Vignale, *Quantum theory of the electron liquid* Ch. 4 (University Press, Chambridge, 2005).